



2



Research and Development Technical Report  
SLCET-TR-91-26 (Rev. 1)

# Low-Noise Oscillators for Airborne Radar Applications

Raymond L. Filler and John R. Vig  
Army Research Laboratory

August 1993

DTIC  
ELECTE  
SEP 14 1993  
S A D

Approved for public release.  
Distribution is unlimited.

ARMY RESEARCH LABORATORY  
Electronics and Power Sources Directorate  
Fort Monmouth, NJ 07703-5601, U.S.A.

93 9 14 105

93-21430



## NOTICES

### Disclaimers

The findings in this report are not to be construed as an official Department of the Army position, unless so designated by other authorized documents.

The citation of trade names and names of manufacturers in this report is not to be construed as official Government indorsement or approval of commercial products or services referenced herein.

# REPORT DOCUMENTATION PAGE

Form Approved  
OMB No. 0704-0188

Public reporting burden for this collection of information is estimated to average 1 hour per response, including the time for reviewing instructions, searching existing data sources, gathering and maintaining the data needed, and completing and reviewing the collection of information. Send comments regarding this burden estimate or any other aspect of this collection of information, including suggestions for reducing this burden, to Washington Headquarters Services, Directorate for Information Operations and Reports, 1215 Jefferson Davis Highway, Suite 1204, Arlington, VA 22202-4302, and to the Office of Management and Budget, Paperwork Reduction Project (0704-0188), Washington, DC 20503.

1. AGENCY USE ONLY (Leave blank)	2. REPORT DATE <p style="text-align: center;">August 1993</p>	3. REPORT TYPE AND DATES COVERED <p style="text-align: center;">Technical Report</p>	
4. TITLE AND SUBTITLE <p style="text-align: center;">Low-Noise Oscillators for Airborne Radar Applications</p>		5. FUNDING NUMBERS <p style="text-align: center;">PE: 1L1 PR: 62705 TA: AH94</p>	
6. AUTHOR(S) <p style="text-align: center;">Raymond L. Filler and John R. Vig</p>		8. PERFORMING ORGANIZATION REPORT NUMBER <p style="text-align: center;">SLCET-TR-91-26 (Rev. 1)</p>	
7. PERFORMING ORGANIZATION NAME(S) AND ADDRESS(ES) Army Research Laboratory Electronics and Power Sources Directorate ATTN: AMSRL-EP-ME Fort Monmouth, NJ 07703-5601		10. SPONSORING/MONITORING AGENCY REPORT NUMBER	
9. SPONSORING/MONITORING AGENCY NAME(S) AND ADDRESS(ES)		11. SUPPLEMENTARY NOTES This report is a revision of Technical Report SLCET-TR-91-26, same title, dated October 1991, AD-A242264. The report is a slightly revised reprint of a paper that appeared in the AGARD Conference Proceedings No. 482, Advances In Components for Active and Passive Airborne Sensors, AGARD-CP-482, which contains the papers presented at the Avionics Panel Specialists Meeting held in Bath, England, 9-10 May 1990.	
12a. DISTRIBUTION/AVAILABILITY STATEMENT <p style="text-align: center;">Approved for public release; Distribution is unlimited.</p>		12b. DISTRIBUTION CODE	
13. ABSTRACT (Maximum 200 words)  Vibration-induced phase noise can change the probability of detection of moving-target indicator (MTI) radar from near-100 percent to zero. Oscillators that are capable of meeting the requirements of MTI radar systems in a quiet environment are readily available. In the vibrating environments of airborne platforms, however, the phase noise of oscillators degrades very significantly. For example, a 10-MHz crystal oscillator may have a phase noise of -140 dBc/Hz, 100 Hz from the carrier. Assuming a typical one part per billion per g acceleration sensitivity, this phase noise degrades to -93 dBc/Hz under a 0.1 sq g/Hz random vibration at 100 Hz away from the carrier. If there is a 1g sinusoidal vibration at 100 Hz, there will be a pair of -86 dBc spectral lines superimposed on the signal. Of course, upon multiplication to 10 GHz, the phase noise increases by at least another 60 dB.  This report reviews the causes and effects of acceleration sensitivity of bulkwave quartz crystal resonators, and the methods that reduce or compensate for that sensitivity. Most of what is discussed is equally relevant to surface acoustic wave (SAW), shallow bulk acoustic wave (SBAW), dielectric resonator-oscillators(DRO), and other types of oscillators.			
14. SUBJECT TERMS Radar, probability of detection, MTI radar, Doppler radar, coherent radar, clock, frequency standard, frequency control, frequency stability, quartz, quartz crystal, quartz oscillator, atomic clock, atomic frequency standard, stability, noise, phase-noise.			15. NUMBER OF PAGES <p style="text-align: center;">20</p>
17. SECURITY CLASSIFICATION OF REPORT <p style="text-align: center;">Unclassified</p>			16. PRICE CODE
18. SECURITY CLASSIFICATION OF THIS PAGE <p style="text-align: center;">Unclassified</p>	19. SECURITY CLASSIFICATION OF ABSTRACT <p style="text-align: center;">Unclassified</p>	20. LIMITATION OF ABSTRACT <p style="text-align: center;">UL</p>	

Table of Contents

	<u>Page</u>
INTRODUCTION .....	1
THE EFFECT OF ACCELERATION ON A CRYSTAL RESONATOR .....	1
THE EFFECT OF VIBRATION ON A CRYSTAL RESONATOR .....	2
FREQUENCY DOMAIN .....	3
SMALL MODULATION INDEX .....	4
FREQUENCY MULTIPLICATION .....	5
LARGE MODULATION INDEX .....	5
ALLAN VARIANCE .....	5
RANDOM VIBRATIONS .....	6
INTEGRATED PHASE NOISE AND PEAK PHASE EXCURSION .....	6
MEASUREMENT .....	8
THEORY .....	8
EXPERIMENTAL RESULTS .....	9
REDUCTION OF THE ACCELERATION SENSITIVITY OF RESONATORS .....	10
MODE SHAPE CONTROL .....	10
ACCELERATION COMPENSATION OF OSCILLATORS .....	11
CONCLUSION .....	12
REFERENCES .....	12

Accession For	
NTIS CRA&I	✓
DTIC TAB	□
Unannounced	□
Justification	
By	
Date	
Availability Codes	
Dist	Availability Codes
A-1	Special

## Figures

<u>Figure</u>		<u>Page</u>
1.	"2-g tipover," frequency change versus rotation in Earth's gravitational field for three mutually perpendicular axes.	2
2.	Instantaneous "carrier" frequency for several instants during one cycle of vibration.	3
3.	(a) Acceleration level versus time. (b) Resulting oscillator output showing frequency modulation.	3
4.	Vibration-induced spectral lines and carrier resulting from sinusoidal acceleration at 5, 25, and 50 Hz.	4
5.	$\sigma_y(\tau)$ versus $\tau$ for an oscillator with acceleration sensitivity of $1 \times 10^{-9}/g$ during 1 g vibration at 20 Hz.	6
6.	Random vibration-induced phase noise and random vibration envelope.	7
7.	Typical equipment configuration for measurement of acceleration-sensitivity using sinusoidal acceleration.	8
8.	Sample acceleration sensitivity measurement results for sinusoidal acceleration.	8

## Tables

<u>Table</u>		
1.	First sideband levels, in dBc, for a 5 MHz oscillator with an acceleration sensitivity of $2 \times 10^{-9}/g$ experiencing an acceleration of 5 g peak.	4
2.	First sideband levels, in dBc, for a 1575 MHz oscillator with an acceleration sensitivity of $2 \times 10^{-9}/g$ experiencing a peak acceleration of 5 g.	5

## INTRODUCTION

Vibration-induced phase noise can change the probability of detection of moving-target indicator (MTI) radar from near-100 percent to zero. Oscillators that are capable of meeting the requirements of MTI radar systems in a quiet environment are readily available. In the vibrating environments of airborne platforms, however, the phase noise of oscillators degrades very significantly. For example, a 10 MHz crystal oscillator may have a phase noise of -140 dBc/Hz, 100 Hz from the carrier, where dBc refers to dB relative to the carrier. Assuming a typical  $1 \times 10^{-9}$  per g acceleration sensitivity, this phase noise degrades to -93 dBc/Hz under a  $0.1 \text{ g}^2/\text{Hz}$  random vibration 100 Hz away from the carrier. If there is a 1g sinusoidal vibration at 100 Hz, there will be a pair of -86 dBc spectral lines superimposed on the signal. Of course, upon multiplication to 10 GHz, the phase noise increases by at least another 60 dB.

There has been an awareness of acceleration effects in frequency sources at least since the advent of missile and satellite applications,<sup>1-6</sup> Doppler radars,<sup>7,8</sup> and other systems requiring extremely low noise.<sup>9,10</sup> There has not, however, been a general appreciation of the magnitude of the problem. As a case in point, there is little or no mention of acceleration sensitivity in the general texts on quartz crystal oscillators and resonators or of vibration-induced phase noise in radar textbooks.

High-stability frequency sources, including atomic standards, contain quartz crystal resonators. One result of the evolution of electronics, i.e., the transition from tubes to transistors, and from point-to-point wiring to printed circuits, is the establishment of the quartz crystal resonator as the most acceleration-sensitive component in frequency sources. This paper reviews the causes and effects of acceleration sensitivity of bulkwave quartz crystal resonators, and the methods that reduce or compen-

sate for that sensitivity. Most of what is discussed is equally relevant to surface acoustic wave (SAW), shallow bulk acoustic wave (SBAW), dielectric resonator-oscillators (DRO), atomic frequency standards, and other types of oscillators.

## THE EFFECT OF ACCELERATION ON A CRYSTAL RESONATOR

A quartz crystal resonator subject to a steady acceleration has a slightly different series resonant frequency than the same resonator experiencing zero acceleration.<sup>1</sup> Furthermore, it has been observed that the magnitude of the frequency shift is proportional to the magnitude of the acceleration, and is also dependent upon the direction of the acceleration relative to a coordinate system fixed to the resonator.<sup>11</sup> It has been shown, empirically, that the acceleration sensitivity of a quartz crystal resonator is a vector quantity.<sup>12</sup> Therefore, the frequency during acceleration can be written as a function of the scalar product of two vectors

$$f(\vec{a}) = f_0 (1 + \vec{\Gamma} \cdot \vec{a}) \quad (1)$$

where  $f(\vec{a})$  is the resonant frequency of the resonator experiencing acceleration  $\vec{a}$ ,  $f_0$  is the frequency with no acceleration (referred to as the carrier frequency), and  $\vec{\Gamma}$  is the acceleration sensitivity vector. It can be seen from Eq. 1 that the frequency of an accelerating resonator is a maximum when the acceleration is parallel to the acceleration sensitivity vector; it is a minimum when the acceleration is antiparallel to the acceleration sensitivity vector. An important result of Eq. 1 is that the frequency shift,  $f(\vec{a}) - f_0$ , is zero for any acceleration in the plane normal to the acceleration sensitivity vector.

The frequency shift described in Eq. 1 is also induced by the acceleration due to gravity (even without motion). This is commonly referred to as "2g-tipover." During "2g-tipover," the magnitude of the acceleration is 1g in the

direction towards the center of the earth. (The magnitude of acceleration given in this paper will be in units of g, i.e., the magnitude of the earth's gravitational acceleration at sea level, 980 cm/sec<sup>2</sup>.) When a resonator is rotated 180° about a horizontal axis, the scalar product of the acceleration and the unit vector normal to the initial "top" of the resonator goes from -1g to +1g, which is a difference of 2g.

Fig. 1 shows actual data of the fractional frequency shift of a resonator (operating in an oscillator) when the oscillator is rotated about three mutually perpendicular axes in the earth's gravitational field. For each curve, the axis of rotation is held horizontal. The sinusoidal shape of each curve is a consequence of the scalar product being proportional to the cosine of the angle between the acceleration sensitivity vector and the acceleration due to gravity.

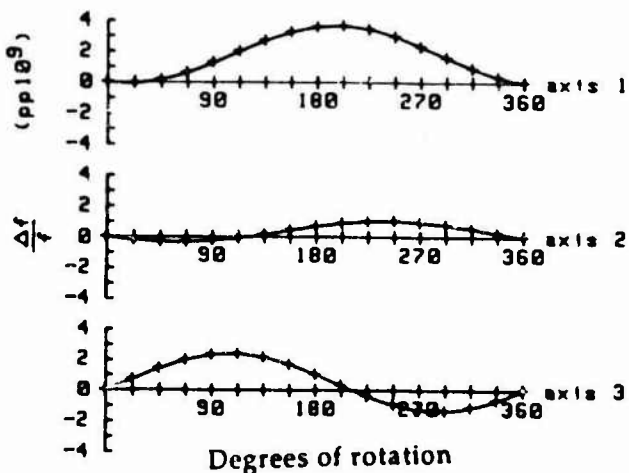


Figure 1. "2-g tipover," frequency change versus rotation in Earth's gravitational field for three mutually perpendicular axes.

#### THE EFFECT OF VIBRATION ON A CRYSTAL RESONATOR

In most applications, the magnitude of the acceleration is time-dependent. The magnitude of the acceleration sensitivity vector, for acceleration amplitudes commonly encountered, is independent of acceleration amplitude.<sup>11</sup> The

time-dependent frequency shift due to a complex vibration can, therefore, be determined from the sum of the individual sinusoidal components, i.e., the system is linear and superposition holds. Simple sinusoidal vibration will be discussed first; the extension will then be made to random vibration.

Simple harmonic motion will be assumed, with an acceleration given by

$$\vec{a} = \vec{A} \cos(2\pi f_v t), \quad (2)$$

where  $\vec{A}$  is the peak acceleration vector in units of g,  $f_v$  is the frequency of vibration in Hertz, and  $t$  is time in seconds. The variation of the frequency with time can be determined by combining Eq. 2 with Eq. 1, resulting in

$$f(\vec{a}) = f_0 (1 + (\vec{\Gamma} \cdot \vec{A}) \cos(2\pi f_v t)). \quad (3)$$

The behavior of the device can be described by defining a rectangular coordinate system fixed to the resonator. The acceleration sensitivity vector and the acceleration vector can then be described in terms of the three unit vectors defined by that coordinate system. Therefore Eq. 3 can be transformed into a scalar equation containing the three (i, j, and k) components of  $\vec{A}$  and  $\vec{\Gamma}$ , i.e.,

$$f(\vec{a}) = f_0 (1 + \Gamma_i A_i + \Gamma_j A_j + \Gamma_k A_k) \cos(2\pi f_v t). \quad (4)$$

This can be rewritten as

$$f(\vec{a}) = f_0 + \Delta f \cos(2\pi f_v t), \quad (5)$$

where

$$\Delta f = f_0 (\Gamma_i A_i + \Gamma_j A_j + \Gamma_k A_k) \quad (6)$$

is the peak frequency shift due to the acceleration  $\vec{A}$ .

There are three quantities with units of frequency to keep in mind:  $f_0$ ,  $f_v$ , and  $\Delta f$ . It can be seen from Eq. 5 that the output frequency deviates from the center frequency,  $f_0$ , by the

amount  $\pm \Delta f$ , at a rate of  $f_v$ . This is shown schematically in Fig. 2.

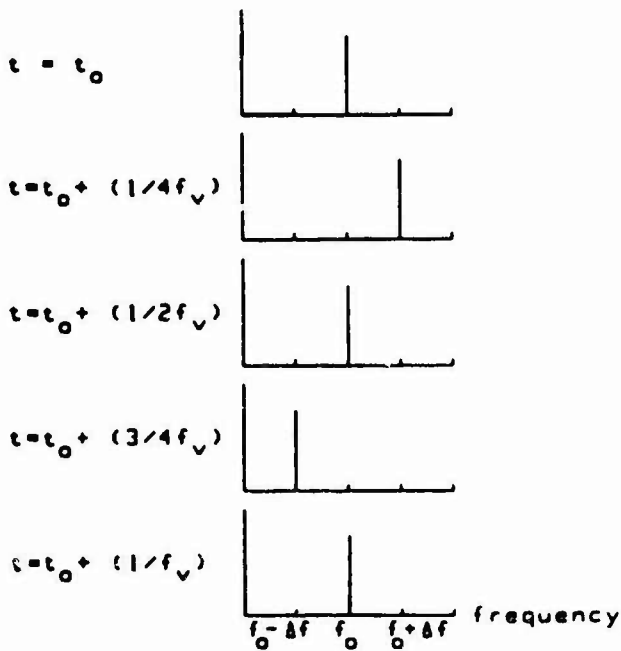


Figure 2. Instantaneous "carrier" frequency for several instants during one cycle of vibration.

Each plot is the instantaneous output frequency of a crystal oscillator while undergoing a vibration at frequency  $f_v$ . Fig. 3b is the voltage versus time at the output of the same crystal oscillator showing, in a much exaggerated way, the variation in the frequency with acceleration amplitude. Fig. 3a is the acceleration waveform.

### FREQUENCY DOMAIN

It is very useful to transform the effect of vibration into the frequency domain. This will allow the formulation of a convenient measurement scheme and allow comparison of vibration effects to more familiar forms of phase noise. The voltage appearing at the output of an oscillator is given by

$$V(t) = V_0 \cos(\phi(t)), \quad (7)$$

where the phase  $\phi(t)$  is derived from the frequency by

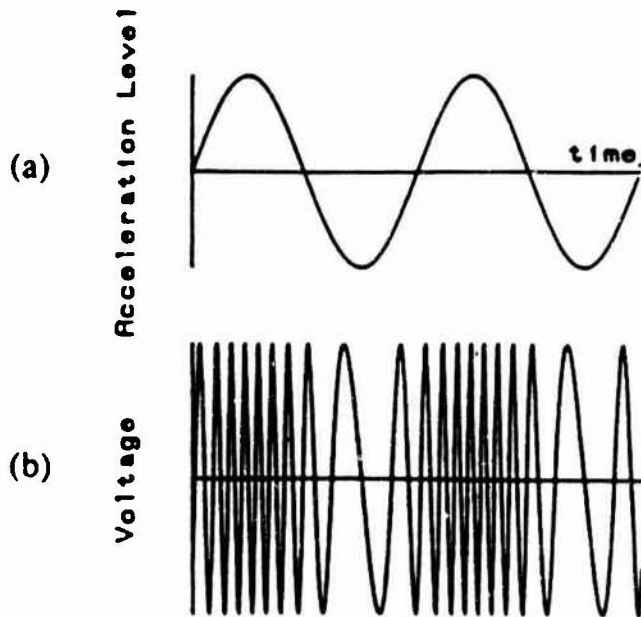


Figure 3. (a) Acceleration level versus time. (b) Resulting oscillator output showing frequency modulation.

$$\phi(t) = 2\pi \int_0^t f(t') dt'. \quad (8)$$

When the oscillator frequency is varying due to simple harmonic acceleration modulating the resonant frequency of the resonator, the phase in Eq. 7 becomes, using Eqs. 5 and 8,

$$\phi(t) = 2\pi f_0 t + (\Delta f/f_v) \sin(2\pi f_v t). \quad (9)$$

When Eq. 9 is inserted into Eq. 7, the result is

$$V(t) = V_0 \cos(2\pi f_0 t + (\Delta f/f_v) \sin(2\pi f_v t)). \quad (10)$$

Eq. 10 is the expression for a frequency-modulated signal. It can be expanded in an infinite series of Bessel functions<sup>13</sup> resulting in<sup>14</sup>

$$V(t) = V_0 [J_0(\beta) \cos(2\pi f_0 t) + J_1(\beta) \cos(2\pi(f_0 + f_v)t) + J_1(\beta) \cos(2\pi(f_0 - f_v)t) + J_2(\beta) \cos(2\pi(f_0 + 2f_v)t) + J_2(\beta) \cos(2\pi(f_0 - 2f_v)t) + \dots] \quad (11)$$

where  $\beta = \Delta f/f_v = (\Gamma \cdot \bar{A})/f_v$  is the modulation index (from standard FM theory).

The first term in Eq. 11 is a sine wave at the carrier frequency with an amplitude, relative to  $V_0$ , of  $J_0(\beta)$ . The other terms are vibration-induced sidebands at frequencies  $f_0 + f_v$ ,  $f_0 - f_v$ ,  $f_0 + 2f_v$ ,  $f_0 - 2f_v$ , etc. (The "sidebands" for sinusoidal vibration are spectral lines, which are also referred to as "brightlines".) The ratio of the power in the  $n$ th vibration-induced sideband to the power in the carrier, denoted by  $I_n(f_v)$ , is given by

$$I_n(f_v) = (J_n(\beta)/J_0(\beta))^2 \quad (12)$$

or, more commonly expressed in decibels as

$$I_n(f_v)(dBc) = 20 \log(J_n(\beta)/J_0(\beta)). \quad (13)$$

### SMALL MODULATION INDEX

Several approximations can be made if the modulation index is less than 0.1. This is the case for most frequency standards in the HF band experiencing "normal" accelerations of 10 g or less at acceleration frequencies above a few hertz. The approximations are

$$\begin{aligned} J_0(\beta) &= 1; & \beta < 0.1 \\ J_1(\beta) &= \beta/2; & \beta < 0.1 \\ J_n(\beta) &= 0; & \beta < 0.1, n > 2. \end{aligned} \quad (14)$$

Therefore, after combining Eqs. 13 and 14:

$$I_1(f_v) = 20 \log((\vec{\Gamma} \cdot \vec{A}) f_0 / (2f_v)) \quad (15)$$

$$I_{n>1}(f_v) = 0$$

For small modulation index, therefore, most of the power is in the carrier and a small amount is in the first sideband pair (upper and lower). The amplitudes of the higher sidebands are negligible.

As an example, consider a 5 MHz oscillator with a vibration sensitivity of  $2 \times 10^9/g$ . If the oscillator experiences an acceleration of 5 g along the direction of the acceleration sensitivity vector, the value of  $\Delta f$  is  $(5 \times 10^9 \text{ Hz}) \cdot (5 \text{ g}) \cdot (2 \times 10^{-9}/g) = 0.05 \text{ Hz}$ . The modulation index

and  $I_1(f_v)$  for several vibration frequencies are shown in Table 1.

TABLE 1

First sideband levels, in dBc, for a 5 MHz oscillator with an acceleration sensitivity of  $2 \times 10^9/g$  experiencing an acceleration of 5 g peak.

$f_v$ (Hz)	$\beta$	$I_1(f_v)$ (dBc)
5	0.01	-46
25	0.002	-60
50	0.001	-66
500	0.0001	-86

It can be seen that  $I_1$  falls off at 6 dB per octave (20 dB per decade.) A consequence of linearity at low vibration levels is that these sinusoidal accelerations are independent. The amplitude at any frequency is the same if the brightlines are excited separately or in combination. The first three of these vibration-induced spectral lines and the carrier are shown in a typical spectrum analyzer output in Fig. 4.

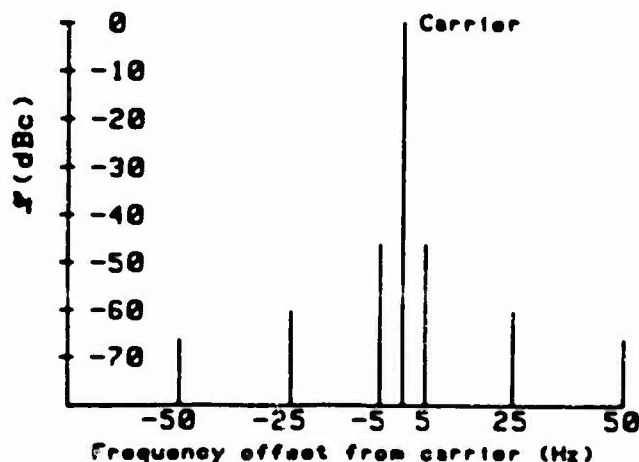


Figure 4. Vibration-induced spectral lines and carrier resulting from sinusoidal acceleration at 5, 25, and 50 Hz.

## FREQUENCY MULTIPLICATION

Phase noise during vibration is of great concern in systems such as radar, navigation, and satellite communications, where the frequency of the crystal oscillator is multiplied up to the microwave region. Upon frequency multiplication by a factor of  $N$ , the vibration frequency  $f_v$  is unaffected since it is an external influence. The peak frequency change due to vibration,  $\Delta f$ , however, becomes

$$\Delta f = (\bar{\Gamma} \cdot \bar{A}) N f_0. \quad (16)$$

The modulation index  $\beta$  is therefore increased by a factor of  $N$ . Expressed in decibels, frequency multiplication by a factor  $N$  increases the phase noise power by  $20 \log N$ .

The relationship between the vibration-induced phase noise power of two oscillators with the same vibration sensitivity and different carrier frequencies is

$$I_B(f_v) = I_A(f_v) + 20 \log(f_B/f_A), \quad (17)$$

where  $I_A(f_v)$  is the sideband level, in dBc, of the oscillator at frequency  $f_A$ , and  $I_B(f_v)$  is the sideband level of the oscillator at frequency  $f_B$ . Frequency multiplication to a higher frequency is indistinguishable from direct frequency generation at the higher frequency. For example, when a  $2 \times 10^{-9}/g$  sensitivity 5 MHz oscillator's frequency is multiplied by a factor of 315 to generate a frequency of 1575 MHz, its output will have identical vibration-induced sidebands to a 1575 MHz SAW oscillator with a sensitivity of  $2 \times 10^{-9}/g$ . This is identical to the "20 log  $N$ " term associated with the increase in phase noise due to frequency multiplication. Again, this relationship holds only if  $\beta < 0.1$ .

## LARGE MODULATION INDEX

If the modulation index  $\beta$  is larger than 0.1, the approximations made in Eq. 14 are not valid. This often occurs in UHF and higher frequency systems.<sup>9</sup> At 5 g acceleration, for example, the

vibration-induced sidebands produced by the 1575 MHz oscillator and the 5 MHz oscillator multiplied by 315 are shown in Table 2.

TABLE 2

First sideband levels, in dBc, for a 1575 MHz oscillator with an acceleration sensitivity of  $2 \times 10^{-9}/g$  experiencing a peak acceleration of 5 g.

$f_v$ (Hz)	$\beta$	$I_1(f_v)$ (dBc)
5.25	3.15	+2.3
25	0.63	-9.6
50	0.315	-16.0
500	0.0315	-36.0

It can be seen that the values of  $I_1(f_v)$  in Table 2 are much greater than those in Table 1 for the same vibration frequency. This is a consequence of the ratio of carrier frequency to vibration frequency being much larger. It is possible, as can be seen in this example, for the sidebands to be larger than the carrier. Also, there are even conditions where the carrier disappears and the value of  $I_1(f_v)$  goes to infinity, e.g., when  $\beta$  equals 2.4, that is, all of the power is in the sidebands and none is in the carrier.

## ALLAN VARIANCE

The effect of sinusoidal phase modulation on the two-sample deviation (also called the square-root of the Allan variance)  $\sigma_y(\tau)$  of a frequency standard has been shown<sup>15</sup> to be

$$\sigma_y = (\Phi / \pi f_0 \tau) \sin^2(\pi f_v \tau) \quad (18)$$

where  $\Phi$  is the peak phase deviation,  $f_v$  is the frequency of the phase modulation, and  $\tau$  is the measurement time. It can be seen from Eq. 9 that the magnitude of the maximum phase deviation for a single vibration-induced sideband is  $\Delta f/f_v$ . Therefore, the vibration-induced

$\sigma_y(\tau)$  of a frequency standard with an acceleration sensitivity of  $\bar{\Gamma}$ , subjected to acceleration  $\bar{A}$  at a frequency of  $f_v$ , is

$$\sigma_y = [(\bar{\Gamma} \cdot \bar{A}) / (\pi f_v \tau)] \sin^2(\pi f_v \tau). \quad (19)$$

This effect is shown in Fig. 5. The frequency standard is assumed to have an Allan variance of  $(1 \times 10^{-12}/\tau)^2$  when not being accelerated.

A plausibility argument for the occurrence of the peaks and valleys in Fig. 5 is that the average frequency, as given in Eq. 5, is  $f_0$  for an averaging time equal to an integer multiple of the period of the vibration. Since this is a constant, the variance is zero. The average frequency departure from  $f_0$  is a maximum when the averaging time is an integer multiple of one-half the period of the vibration. Therefore, the peaks in Fig. 5 occur when  $\tau = (2n + 1)/(2f_v)$  and the valleys occur when  $\tau = (n + 1)/f_v$ , where  $n = 0, 1, 2, 3, \dots$

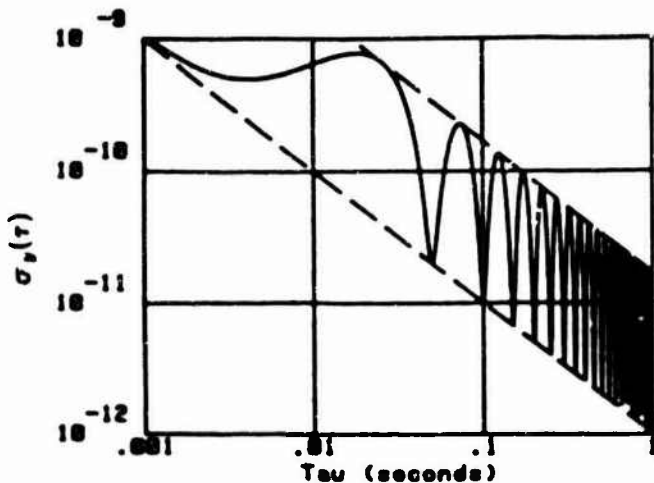


Figure 5.  $\sigma_y(\tau)$  versus  $\tau$  for an oscillator with acceleration-sensitivity of  $1 \times 10^{-9}/g$  during  $1 g$  vibration at  $20 \text{ Hz}$ .

## RANDOM VIBRATIONS

In most situations the acceleration experienced by a frequency standard is not simple harmonic motion; it is random, i.e., the vibratory power is randomly distributed over a range of frequencies, phases, and amplitudes. The accelera-

tion can be described by its power spectral density  $G(f)$ . The power spectral density of frequency fluctuations,  $S_y(f)$ , can be obtained by multiplying the power spectral density of acceleration by the square of the acceleration sensitivity in  $(\text{Hz}/g)^2$ . The single-sideband measure of stability,  $\mathcal{L}(f)$ , is related to  $S_y(f)$ , if the modulation index is small, by<sup>18</sup>

$$\mathcal{L}(f) = S_y(f) / (2f^2). \quad (20)$$

Therefore,  $\mathcal{L}(f)$  for random vibration is given by

$$\mathcal{L}(f) = (\bar{\Gamma} / f_0)^2 G(f) / (2f^2). \quad (21)$$

As an example, consider the random acceleration spectrum given in the upper right of Fig. 6.  $G(f)$ , in units of  $g^2/\text{Hz}$ , is given by

$$\begin{aligned} G(f) &= 0.04 & 5 < f < 220 \text{ Hz} \\ G(f) &= 0.07 * (f/300)^2 & 220 < f < 300 \text{ Hz} \\ G(f) &= 0.07 & 300 < f < 1000 \text{ Hz} \\ G(f) &= 0.07 * (f/1000)^2 & 1 < f < 2 \text{ kHz} \end{aligned} \quad (22)$$

If the vibration sensitivity is  $1 \times 10^{-9}/g$  and the oscillator is operating at  $10 \text{ MHz}$ , the peak frequency deviation is  $0.01 \text{ Hz}$ . Therefore,  $\mathcal{L}(f)$  is

$$\mathcal{L}(f) = \begin{cases} \left( \frac{(0.04) * (0.01)^2}{2f^2} \right) & 5 < f < 220 \text{ Hz} \\ \left( \frac{0.07}{2} \right) \left( \frac{0.01}{300} \right)^2 & 220 < f < 300 \text{ Hz} \\ \left( \frac{(0.07)(0.01)^2}{2f^2} \right) & 300 < f < 1000 \text{ Hz} \\ \left( \frac{(0.07)(0.01/1000)^2}{2f^2} \right) & 1 < f < 2 \text{ kHz} \end{cases} \quad (23)$$

which is shown in Fig. 6. Note that outside of the vibration frequency range defined by the given acceleration spectrum, the phase noise is identical to that of a non-accelerated device.

## INTEGRATED PHASE NOISE AND PEAK PHASE EXCURSION

Specialists in crystal resonators and oscillators generally characterize phase noise by  $S_y(f)$  or  $\mathcal{L}(f)$ . Many users of crystal oscillators, howev-

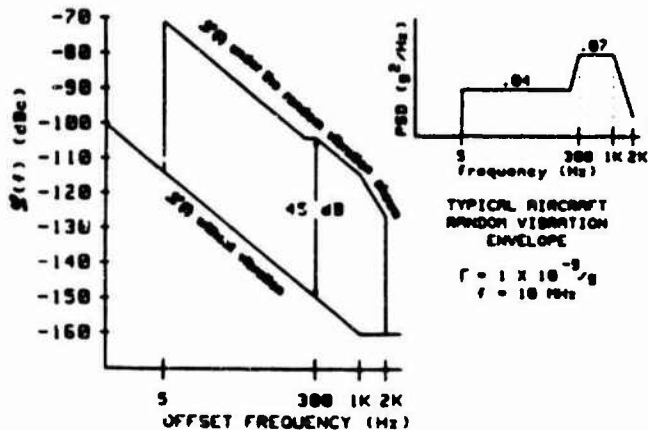


Figure 6. Random vibration-induced phase noise and random vibration envelope.

er, characterize phase noise in terms of "phase jitter." Phase jitter is the phase noise integrated over the system bandwidth. Similarly, in phase-lock-loops, it is the magnitude of the phase excursions that determines whether or not the loop will break lock under vibration.

One can use the previous example to investigate the effect of vibration on integrated phase noise. Integrated phase noise is defined, for the band  $f_1$  to  $f_2$ , as

$$\Phi_i^2 = \int_{f_1}^{f_2} S_\phi(f) df, \quad (24)$$

where  $S_\phi$  is the spectral density of phase, equal to  $2 \mathcal{L}$  in the frequency band of 1 Hz to 2 KHz, the phase noise of the nonvibrating oscillator from Fig. 6 is given by

$$\begin{aligned} \mathcal{L} &= 1 \times 10^{-10} / f^2 & f \leq 1 \text{ kHz} \\ \mathcal{L} &= 1 \times 10^{-16} & f \geq 1 \text{ kHz} \end{aligned} \quad (25)$$

and the integrated phase noise in the same band is

$$\Phi_i^2 = 2 \times 20^{-10} \text{ radians}^2. \quad (26)$$

Therefore,

$$\Phi_i = 1.4 \times 10^{-5} \text{ radians}. \quad (27)$$

While the oscillator is vibrating, the phase noise is given by Eq. 25 in the band from 1 Hz to 5 Hz, and by Eq. 23 in the band from 5 Hz to 2000 Hz. The integrated phase noise is

$$\begin{aligned} \Phi_i^2 &= 2 \int_1^5 \left( \frac{1 \times 10^{-10}}{f^2} \right) df + \int_5^{220} \frac{(0.04)(0.01)^2}{f^2} df \\ &+ \int_{220}^{300} (0.07) \left( \frac{0.01}{300} \right)^2 df + \int_{300}^{1000} \frac{(0.07)(0.01)^2}{f} df \\ &+ \int_{1000}^{2000} \frac{(0.07)(0.01 \cdot 1000)^2}{f^2} df \\ &= 8 \times 10^{-7} \text{ radians}^2. \end{aligned} \quad (28)$$

Therefore,

$$\Phi_i = 9 \times 10^{-4} \text{ radians}. \quad (29)$$

While the oscillator is vibrating, it can be seen that the integrated phase noise is 4000 times that of the noise when it is not vibrating and the rms phase deviation,  $\Phi_i$ , is about 60 times larger during vibration.

When the oscillator is subjected to a simple sinusoidal vibration, the peak phase excursion follows from Eq. 9, i.e.,

$$\Phi_{\text{peak}} = \Delta f / f_v. \quad (30)$$

For example, if our 10 MHz,  $1 \times 10^{-9}/g$  oscillator is subjected to a 10 Hz sinusoidal vibration of amplitude 1 g, the peak vibration-induced phase excursion is  $1 \times 10^{-3}$  radians. If this oscillator is used as the reference oscillator in a 10 GHz radar system, the peak phase excursion at 10 GHz will be 1 radian. Similarly, when an oscillator's frequency is multiplied, the square root of the integrated phase noise is increased by the multiplication factor. At 10 GHz, for example,  $\Phi_i$  in the above example increases from  $9 \times 10^{-4}$  radians to 0.9 radians! Such large phase excursions are detrimental to the performance of many systems, such as those which employ phase lock loops or phase shift keying.

## MEASUREMENT

The sidebands generated by vibration can be used to measure the acceleration sensitivity. Eq. 15 can be rearranged to get

$$\Gamma_i = (2f_v/A_i f_o) 10^{(L_i)/20}, \quad (31)$$

where  $\Gamma_i$  is the component of the acceleration sensitivity vector in the  $i$  direction. Three measurements, along mutually perpendicular axes, are required to characterize  $\vec{\Gamma}$ , which becomes

$$\vec{\Gamma} = \Gamma_i \hat{i} + \Gamma_j \hat{j} + \Gamma_k \hat{k} \quad (32)$$

with a magnitude of

$$|\vec{\Gamma}| = (\Gamma_i^2 + \Gamma_j^2 + \Gamma_k^2)^{1/2}. \quad (33)$$

One scheme for measuring  $\vec{\Gamma}$  is shown in Fig. 7. The local oscillator is used to mix the carrier frequency down to the range of the spectrum analyzer. If the local oscillator is not modulated, the relative sideband levels are unchanged

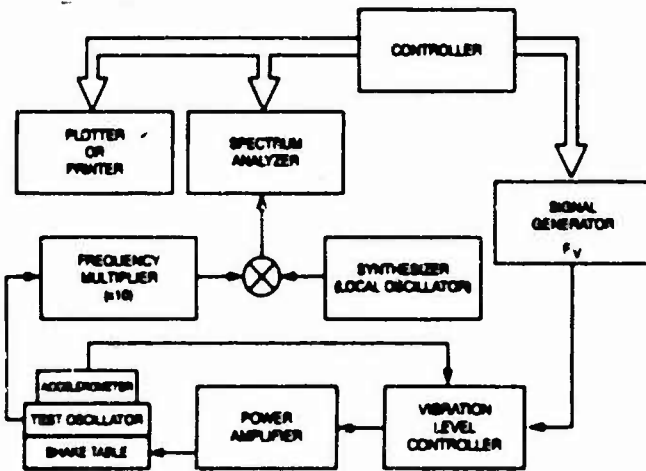


Figure 7. Typical equipment configuration for measurement of acceleration sensitivity using sinusoidal acceleration.

by mixing. The frequency multiplier is used to overcome dynamic range limitations of the spectrum analyzer, using the "20 log N" enhancement discussed previously. The mea-

sured sideband levels must be adjusted for the multiplication factor prior to insertion into Eq. 31. It must be stressed that Eq. 17 is valid only if  $\beta < 0.1$ . A sample measurement output and calculation is given in Fig. 8.

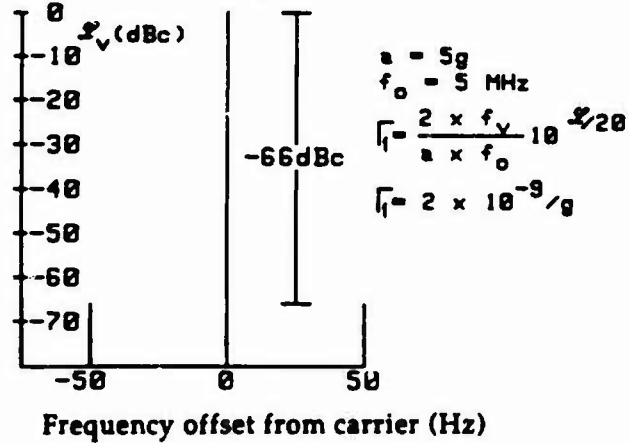


Figure 8. Sample acceleration-sensitivity measurement results for sinusoidal acceleration.

Other measurement schemes include passive excitation<sup>17</sup> of the resonator, the use of random vibration,<sup>18</sup> and the 2-g tipover test. Many oven-controlled oscillators are not suitable for characterization by the 2-g tipover test, however, because rotation of the oscillator results in temperature changes inside the oven that can mask the effects due to the acceleration changes. Vibration tests are also subject to pitfalls since resonances in the oscillator or shake table assembly can produce false results. It is, therefore, important to perform the test at more than one frequency.

## THEORY

The theoretical understanding of acceleration sensitivity does not yet enable one to predict the acceleration sensitivity of "real" resonator designs. Theoretical activity started with the study of in-plane forces on simplified resonator models. The first studies were concerned with the closely related force-frequency effect. This effect, first reported by Bottom<sup>19</sup> in 1947, is the

change in frequency induced by a pair of opposed forces in the plane of a resonator plate applied at the rim. Those forces distort the quartz plate and, because of the nonlinear elastic behavior, change the acoustic velocity.<sup>11</sup> Since the frequency of a resonator is a function of the acoustic velocity and the dimensions of the quartz plate, the forces change the frequency.

The first attempt at an analytical solution to the force-frequency problem was made by Mingins, Barcus, and Perry in 1962.<sup>20</sup> They assumed an AT-cut crystal plate of infinite lateral dimension and used a perturbation technique with linear elastic coefficients. In 1963, they discussed nonlinear theory and the need to include the third-order elastic coefficients.<sup>21</sup> Those coefficients were measured in 1966 by Thurston, McSkimin, and Andreatch.<sup>22</sup> The first calculation to use the nonlinear theory was performed by Keyes and Blair in 1967.<sup>23</sup> In 1973, Lee, Wang, and Markenscoff<sup>24</sup> published the first of a continuing series of papers (by Lee and his students), in which they calculated the force-frequency coefficient (as defined by Ratajski<sup>25</sup>) as a function of azimuth, using the general theory of incremental elastic deformations superimposed on finite initial deformations. The next year, Lee et al investigated the frequency change due to cantilever bending of the plate.<sup>26</sup> In 1977, a variational analysis of the force-frequency effect, including the effect of material anisotropy on initial stress, was given by EerNisse, Ballato, and Lukaszek<sup>27</sup> for doubly rotated cuts. In 1978, Janiaud, Nissim, and Gagnepain<sup>28</sup> obtained analytic solutions for the biasing stress in singly and doubly rotated plates subject to diametric forces. Those results allowed them to calculate Ratajski's force-frequency coefficient, and also the in-plane acceleration sensitivity. Lee and Wu<sup>29</sup> extended the work of reference 24 to treat plates of any cut. In that paper, the solution for an arbitrary number of ribbon supports was obtained.

Under acceleration, body forces in the quartz plate are balanced by reaction forces from the mounting structure. As in the force-frequency effect, distortion of the crystal lattice causes the resonant frequency to change. For bulkwave resonators, only the in-plane case has been treated. The first analysis was by Valdois, Besson, and Gagnepain<sup>11</sup> in 1974, who showed that the effect is linear. Several papers by Lee and Wu<sup>29-31</sup> considered resonators with three- and four-point mounts. Two-point mounts were considered by Janiaud, Nissim, and Gagnepain.<sup>28</sup> For SAW resonators, recent work by Shick and Tiersten<sup>32</sup> and by Sinha and Locke<sup>33</sup> has treated acceleration both in the plane of the plate and normal to it.

There seems to be a significant dependence of the acceleration sensitivity on small variations in the mounting. Analyses of bulkwave resonators, to date, have considered only point supports. Real resonators have supports that are distributed over a finite area. In addition, initial stress conditions are difficult to determine and may not be well-reproduced. There is an ongoing effort by Lee and Tang<sup>34</sup> to use finite element analysis to more accurately model the mounting structure. It is hoped that this will allow computer simulations that will permit the determination of the optimum design parameters for minimizing acceleration sensitivity.

## EXPERIMENTAL RESULTS

Several papers have reported experimental results on the force-frequency effect<sup>20,25,35</sup> and the effects of bending moments.<sup>36</sup> All used point mounts in special fixtures, and results agree fairly well with the theoretical analyses. The reported experimental observations of the actual acceleration sensitivity of real resonators, on the other hand, is remarkable in that it defies simple explanation.

The experimental effort on acceleration sensitivity started in the 1960's with Smith, Spencer,

and Warner.<sup>1-5</sup> Valdois, Besson, and Gagnepain<sup>11</sup> made measurements on resonators and oscillators to demonstrate that the resonator was the acceleration-sensitive element. Results from 2-g tipover experiments were reported for SC-cut resonators by Kusters, Adams, Yoshida, and Leach<sup>37</sup> in 1977. In 1979, Warner, Goldfrank, Meirs, and Rosenfeld<sup>38</sup> reported results on SC- and FC-cut devices. In 1981, the first of a series of papers intended to explore a wide range of resonator fabrication parameters was published by Filler and Vig.<sup>39</sup> In that same year, Nakazawa, Lukaszek, and Ballato<sup>40</sup> reported constant-acceleration results that suggested an acceleration sensitivity that is not linear with acceleration level. A significant parameter for the reduction of acceleration sensitivity was reported by Filler, Kosinski, and Vig<sup>41</sup> in 1982. As one makes plano-convex and biconvex AT-cut resonators flatter, the acceleration sensitivity decreases. It must be noted, however, that other effects, possibly due to insufficient "mode shape control" (see section on that subject below), caused large scatter in the data. A survey of a large number of resonator parameters, such as SC-cut contour, thickness, drive level, temperature, and angle of cut, was published in 1983 by Filler, Kosinski, and Vig.<sup>42</sup> No significant correlations were found.

A paper, by Weglein<sup>43</sup> in 1984, reported the acceleration sensitivity of VHF AT- and SC-cut resonators. All of the resonators in that study were disassembled after the acceleration sensitivity measurements to examine fabrication details. That investigation, which seems to summarize the efforts to date, showed "little dependence on any recognizable parameter," except that the lowest average acceleration sensitivity was found in the group of AT units. The large spread in the data, typical of all experimental observations of acceleration sensitivity, seems to be caused by a combination of sometimes offsetting subtle effects, which are difficult to control during fabrication.

## REDUCTION OF THE ACCELERATION SENSITIVITY OF RESONATORS

The introduction of the stress-compensated cut of quartz, i.e., the SC-cut, was accompanied by the widespread expectation that the SC-cut would have significantly lower acceleration sensitivity than other cuts. Unfortunately, that expectation has not been realized. The lowest acceleration sensitivity achieved with AT-cut resonators<sup>41-43</sup> equals that achieved with SC-cut resonators; both cuts can have low parts in  $10^{10}$ /g sensitivity.

Efforts to reduce the sensitivity of individual resonators to the effects of acceleration have stressed the support structure. Lukaszek and Ballato<sup>44</sup> proposed a plate geometry that would assure the proper support configuration to reduce the force-frequency effect. Besson, Gagnepain, Janiaud, and Valdois<sup>45</sup> proposed a support structure that insured symmetry with the median plane of the resonator plate. Debaisieux, Aubry, and Gros Lambert<sup>46</sup> and Aubry and Debaisieux<sup>47</sup> have reported results using QAS resonators, a variation of the BVA,<sup>48</sup> which insures symmetry of mount as well as accurate mount locations for reducing the force-frequency effect. Their results show a marked reduction in the scatter of the measured acceleration sensitivity.

## MODE SHAPE CONTROL

Recent theoretical and experimental evidence by EerNisse, et al.,<sup>49,50</sup> and Tiersten and Zhou<sup>51</sup> indicates that the major variable yet to be controlled properly is the shape and location of the mode (active region of vibration) in a "real world" resonator. Theoretically, it can be shown that the frequency shift due to a stress on the resonator, such as that caused by acceleration, is given by the integral of the third-order elastic constant times the mode energy density times the strain pattern set up by the acceleration. Leaving out tensor notation, for simplicity,

$$\Delta f/f = C_3 \int_V G^2(X,Y,Z) E(X,Y,Z) dV \quad (34)$$

where  $\Delta f/f$  is fractional frequency shift,  $G$  is the normalized strain distribution associated with the mode of vibration ( $G^2$  is proportional to the strain energy density),  $E$  is the strain distribution associated with the stress caused by acceleration,  $C_3$  is the third-order elastic constant tensor,  $V$  is the volume of the resonator, and  $dV = dXdYdZ$ .

EerNisse showed that very small changes in the mode shape and location have significant effects on the integral, i.e., on the acceleration sensitivity of resonators. He further argued that, because of material imperfections (such as dislocations), and fabrication imperfections (thickness variations, contouring flaws, electrode mass density and thickness variations), the demands on mode shape control will be impractical to accomplish during manufacturing without some ability to "trim" the mode shape and location for each individual resonator. He was able to produce changes in the acceleration sensitivity of resonators by depositing platinum on selected areas of resonators (in order to change the mode shape and location).

#### ACCELERATION COMPENSATION OF OSCILLATORS

The lack of progress in reducing the acceleration sensitivity of the resonator below the low parts in  $10^{10}/g$  level has spawned several techniques for compensation of the effect. There are two general classes of compensation, passive and active. The first compensation results were published by Gagnepain and Walls in 1977.<sup>52</sup> They used the passive method of mechanically arranging two resonators such that the components of the acceleration sensitivities normal to the plates were antiparallel. The resonators were electrically connected in series in a single oscillator. Przyjemski<sup>12</sup> and Emmons<sup>53</sup> used an active technique. They sensed the acceleration

magnitude with an accelerometer aligned with the direction of the acceleration sensitivity vector of the resonator. The accelerometer signal was fed into a tuning circuit in the oscillator in order to counter the acceleration-induced frequency changes. A limitation of this technique is the requirement on the linearity of the tuning network at all operating points. Emmons also employed the dual-resonator technique and suggested using an acceleration-sensitive capacitor in the tuning network of the oscillator. The latter technique is available as an option on a commercial cesium-beam frequency standard.

Ballato<sup>54</sup> suggested a method for compensation in all directions using a resonator pair made of enantiomorphs. He argued that opposite-handedness is the only way to line up all three crystallographic axes to be antiparallel. This was extended by a series of patents by Ballato and Vig.<sup>55-57</sup> A simplification was patented by Filler,<sup>58</sup> who showed that, since the acceleration sensitivity has vector properties, all that is required is that the vectors be aligned antiparallel, independent of the handedness of the quartz. Vig and Walls<sup>59</sup> extended this work by suggesting a method to accommodate resonators with different acceleration sensitivity magnitudes.

Rosati patented<sup>60</sup> an active technique of compensation which was further developed by Rosati and Filler.<sup>61</sup> This method makes use of the polarization effect in doubly rotated resonators, i.e., that the resonant frequency of a doubly rotated resonator is a function of the voltage applied to the electrodes.<sup>62</sup> If one senses the acceleration using an accelerometer and feeds that signal with appropriate amplification and phase reversal directly to the resonator electrodes, compensation can be achieved. The advantage of feeding the correction signal to the resonator electrodes rather than a varactor is that the polarization effect has superior linearity. When the correction signal is applied to a varactor, the nonlinearity

of the varactor and of the frequency-capacitance function causes sidebands at harmonics of the vibration frequency. One implementation of this technique was used to compensate a rubidium oscillator.<sup>63</sup> A refinement was proposed by Frerking.<sup>64</sup>

## CONCLUSION

Vibration effects are a significant problem in modern communication, navigation, and radar systems. Progress has been made in understanding the causes of acceleration sensitivity but achieving less than a few parts in  $10^{10}$  per g has been elusive. Mode shape control may allow significant improvements in the future. A great deal of effort has been expended on compensating for acceleration sensitivity, but more work is needed to improve the level and bandwidth of the compensation.

An IEEE committee has prepared a report which reviews "The Effects of Acceleration on Precision Frequency Sources," and provides guidelines for the specification and testing of oscillator acceleration sensitivities.<sup>65,66</sup>

## REFERENCES

1. A. W. Warner and W. L. Smith, "Quartz Crystal Units and Precision Oscillators for Operation in Severe Mechanical Environments," 14th ASFC, pp 200-216, 1960.
2. W. L. Smith, "An Ultra-Precise Standard of Frequency," Final Report, Contract DA 36-039 SC-73078, US Army, 1960.
3. W. J. Spencer and W. L. Smith, "Precision Crystal Frequency Standards," 15th ASFC, pp 139-155, 1961.
4. W. J. Spencer and W. L. Smith, "Precision Quartz Crystal Controlled Oscillator for Severe Environmental Conditions," 16th ASFC, pp 406-421, 1962.
5. W. L. Smith and W. J. Spencer, "Quartz Crystal Controlled Oscillators," Final Report, Contract DA 36-039 SC-85373, US Army, 1963.
6. D. B. Leeson, "Aerospace Crystal Environmental Requirements," 19th ASFC, pp 49-57, 1965.
7. D. B. Leeson and G. F. Johnson, "Short-Term Stability for a Doppler Radar: Requirements, Measurements, and Techniques," Proc. IEEE, 54, pp 244-248, 1966.
8. G. F. Johnson, "Vibration Characteristics of Crystal Oscillators," 21st ASFC, pp 287-293, 1967.
9. J. Moses, "NAVSTAR Global Positioning System Oscillator Requirements for the GPS Manpack," 30th ASFC, pp 390-400, 1967.
10. J. M. Przyjemski and P. L. Konop, "Limitations on GPS Receiver Performance Imposed by Crystal-Oscillator g-Sensitivity," NAECON '77, 1977.
11. M. Valdois, J. Besson, and J. J. Gagnepain, "Influence of Environment Conditions on a Quartz Resonator," 28th ASFC, pp 19-32, 1974.
12. J. M. Przyjemski, "Improvement in System Performance using a Crystal Oscillator Compensated for Acceleration Sensitivity," 32nd ASFC, pp 426-431, 1978.
13. M. Abramowitz and I. A. Stegun, "National Bureau of Standards, Applied Mathematics Series, No. 55," Government Printing Office, Washington, DC, 1964. Revised by Dover, New York, 1965.
14. R. L. Filler, "The Effect of Vibration on Frequency Standards and Clocks," 35th ASFC, pp 31-39, 1981.

15. S. Stein, private communication, 1986. using eq. 23 from Barnes et. al., "Characterization of Frequency Stability," IEEE Trans. IM, vol. IM-20, 1971.
16. D. Halford, J. S. Shoaf, and A. S. Risley, "Spectral Density Analysis: Frequency Domain Specification and Measurement of Signal Stability," 27th ASFC, pp 421-431, 1973.
17. F. L. Walls and A. E. Wainwright, "Measurement on the Short-term Stability of Quartz Crystal Resonators and the Implication for Crystal Oscillator Design," IEEE Trans. on I&M, IM-24, pp 15-20, 1975.
18. D. J. Healy, III, H. Hahn, and S. Powell, "A Measurement Technique for Determination of Frequency vs. Acceleration Characteristics of Quartz Crystal Units," 37th ASFC, pp 284-289, 1983.
19. V. Bottom, "Note on the Anomalous Thermal Effect in Quartz Oscillator Plates," American Mineralogist, Vol. 32, pp 590-591, Sept - Oct 1947.
20. C. R. Mingins, L. C. Barcus, and R. W. Perry, "Effects of External Forces on the Frequency of Vibrating Crystal Plates," 16th ASFC, pp 47-76, 1962.
21. C. R. Mingins, L. C. Barcus, and R. W. Perry, "Reactions of a Vibrating Piezoelectric Plate to Externally Applied Forces," 17th ASFC, pp 51-87, 1963.
22. R. N. Thurston, H. J. McSkimin, and P. Andreatch, Jr., "Third-Order Elastic Coefficients of Quartz," J. Applied Phys. vol 37, pp 267-275, January 1966.
23. R. W. Keyes and F. W. Blair, "Stress Dependence of the Frequency of Quartz Plates," Proc. IEEE (letters), pp 565-566, 1967.
24. P. C. Y. Lee, Y. S. Wang, and X. Markenscoff, "Elastic Waves and Vibrations in Deformed Crystal Plates," 27th ASFC, pp 1-6, 1973.
25. J. M. Ratajski, "The Force Sensitivity of AT-Cut Quartz Crystals," 20th ASFC, pp 33-48, 1966.
26. P. C. Y. Lee and Y. S. Wang, "Effects of Initial Bending on the Resonance Frequencies of Crystal Plates," 28th ASFC, pp 14-18, 1974.
27. A. Ballato, E. P. EerNisse, and T. Lukaszek, "The Force-Frequency Effect in Doubly Rotated Quartz Plates," 31st ASFC, pp 8-16, 1977 or E. P. EerNisse, T. Lukaszek, and A. Ballato, "Variational Calculation of Force-Frequency Constants of Doubly Rotated Quartz Resonators," IEEE Trans. Sonics & Ultrason., Vol. SU-25, No. 3, pp 132-138, May 1978.
28. D. Janiaud, L. Nissim, and J.-J. Gagnepain, "Analytical Calculation of Initial Stress Effects on Anisotropic Crystals Application to Quartz Resonators," 32nd ASFC, pp 169-179, 1978.
29. P. C. Y. Lee and K. M. Wu, "Nonlinear Effect of Initial Stresses in Doubly - Rotated Resonator Plates," 34th ASFC, pp 403-411, 1980.
30. P. C. Y. Lee and K. M. Wu, "Effects of Acceleration on the Resonance Frequencies of Crystal Plates," 30th ASFC, pp 1-7, 1976.
31. P. C. Y. Lee and K. M. Wu, "The Influence of Support Configuration on the Acceleration Sensitivity of Quartz Resonator Plates," 31st ASFC, pp 29-34, 1977.
32. D. V. Shick and H. F. Tiersten, "An Analysis of the Acceleration Sensitivity of ST-Cut Quartz Surface Wave Resonators Supported along the Edges," 40th ASFC, pp 262-268, 1986.

33. B. K. Sinha and S. Locke, "Acceleration and Vibration Sensitivity of SAW Devices," IEEE Trans. on UFFC, vol UFFC-34, 1, pp 29-38, January 1987.
34. P. C. Y. Lee and M. S. H. Tang, "Initial Stress Field and Resonance Frequencies of Incremental Vibrations in Crystal Resonators by Finite Element Method," 40th ASFC, pp 152-160, 1986.
35. A. D. Ballato, "Effects of Initial Stress on Quartz Plates Vibrating in Thickness Modes," 14th ASFC, pp 89-114, 1960.
36. E. D. Fletcher and A. J. Douglas, "A Comparison of the Effects of Bending Moments on the Vibrations of AT and SC (or TTC) Cuts of Quartz," 33rd ASFC, pp 346-350, 1979.
37. J. A. Kusters, C.A. Adams, H. Yoshida, and J. G. Leach, "TTC's - Further Developmental Results," 31st ASFC, pp 3-7, 1977.
38. A. Warner, B. Goldfrank, M. Meirs, and M. Rosenfeld, "Low 'g' Sensitivity Crystal Units and Their Testing," 33rd ASFC, pp 306-310A, 1979.
39. R. L. Filler and J. R. Vig, "The Acceleration and Warmup Characteristics of Four - Point - Mounted SC and AT-Cut Resonators," 35th ASFC, pp 110-116, 1981.
40. M. Nakazawa, T. Lukaszek, and A. Ballato, "Force- and Acceleration-Frequency Effects in Grooved and Ring - Supported Resonators," 35th ASFC, pp 71-91, 1981.
41. R. L. Filler, J. A. Kosinski, and J. R. Vig, "The Effect of Blank Geometry on the Acceleration Sensitivity of AT & SC-Cut Quartz Resonators," 36th ASFC, pp 215-219, 1982.
42. R. L. Filler, J. A. Kosinski, and J. R. Vig, "Further Studies on the Acceleration Sensitivity of Quartz Resonators," 37th ASFC, pp 265-271, 1983.
43. R. D. Weglein, "The Vibration Sensitivity of VHF Quartz Crystals for Missile Applications," 38th ASFC, pp 73-79, 1984.
44. T. J. Lukaszek, and A. Ballato, "Resonators for Severe Environments," 33rd ASFC, pp 311-321, 1979.
45. R. Besson, J.-J. Gagnepain, D. Janiaud, and M. Valdois, "Design of a Bulk Wave Quartz Resonator Insensitive to Acceleration," 33rd ASFC, pp 37-345, 1979.
46. A. Debaisieux, J. P. Aubry, and J. Gros Lambert, "Design of SC Cut 10 MHz H.Q. Crystals with g Sensitivity Better than  $2 \cdot 10^{-10}/g$ ," Proc. 15th Proc. Time & Time Int. Conf. (PTTI), pp 635-650, 1983.
47. J. P. Aubry and A. Debaisieux, "Further Results on 5 MHz and 10 MHz Resonators with BVA and QAS Designs," 38th ASFC, pp 190-200, 1984.
48. R. J. Besson, "A New Piezoelectric Resonator Design," 30th ASFC, pp 78-83, 1976.
49. E. P. EerNisse, L. D. Clayton, and M. H. Watts, "Variational Method for Modeling Static and Dynamic Stresses in a Resonator Disc with Mounts," 43rd ASFC, pp 377-387, 1989.
50. E. P. EerNisse, R. W. Ward, and O. L. Wood, "Acceleration-Induced Frequency Shifts in Quartz Resonators," 43rd ASFC, pp 388-395, 1989.
51. H. F. Tiersten and Y. S. Zhou, "On the Influence of a Fabrication Imperfection on the In-Plane Acceleration Sensitivity of Contoured Quartz Resonators with Rectangular Supports," Proc. 45th ASFC, in press, 1991.

52. J.-J. Gagnepain and F. L. Walls, "Quartz Crystal Oscillators with Low Acceleration Sensitivity," NBSIR 77-855, National Bureau of Standards, 1977.
53. D. A. Emmons, "Acceleration Sensitivity Compensation in High Performance Crystal Oscillators," 10th Prec. Time & Time Int. Conf. (PTTI), 1978.
54. A. Ballato, "Crystal Resonators with Increased Immunity to Acceleration Fields," IEEE Trans. Sonics & Ultrason., Vol SU-27, No. 4, pp 195-201, July 1980; or "Resonators Compensated for Acceleration Fields," 33rd ASFC, pp 322-336, 1979.
55. A. Ballato and J. R. Vig, "Acceleration Resistant Combination of Opposite - Handed Piezoelectric Crystals," US Patent No. 4,344,010, 1982.
56. A. Ballato and J. R. Vig, "Method of Fabricating Acceleration Resistant Resonators, Resonators so Formed," US Patent No. 4,365,182, 1982.
57. A. Ballato and J. R. Vig, "Method of Fabricating Acceleration Resistant Crystal Resonators," US Patent No. 4,409,711, 1983.
58. R. L. Filler, "Acceleration Resistant Crystal Resonators," US Patent No. 4,410,822, 1983.
59. J. R. Vig and F. L. Walls, "Acceleration Insensitive Oscillator," US Patent No. 4,575,690, 1986.
60. V. J. Rosati, "Suppression of Vibration Effects on Piezoelectric Crystal Resonators," US Patent No. 4,453,141, 1984.
61. V. J. Rosati and R. L. Filler, "Reduction of the Effects of Vibration on SC-Cut Quartz Crystal Oscillators," 35th ASFC, pp 117-121, 1981.
62. J. Kusters, "The Effect of Static Electric Fields on the Elastic Constants of Alpha Quartz," 24th ASFC, pp 46-54, 1970.
63. C. Colson, "Vibration Compensation of the Seektalk Rubidium Oscillator," 36th ASFC, pp 197-199, 1982.
64. M. E. Frerking, "Vibration Compensated Crystal Oscillator," U.S. Patent No. 4,891,611, Jan. 2, 1990.
65. J. R. Vig, et al., "The Effects of Acceleration on Precision Frequency Sources," Research and Development Technical Report, SLCET-TR-91-3 (Rev. 1), July 1992; copies available from NTIS.
66. J. R. Vig, et al. "Acceleration, Vibration and Shock Effects," Proc. 1992 IEEE Frequency Control Symposium, in press, IEEE Cat. No. 92CH3083-3, 1992.

---

\*ASFC is the Proceedings of the Annual Symposium on Frequency Control. For the years 1956 to 1988, copies are available from:

National Technical Information Service  
5285 Port Royal Rd.  
Sills Bldg.  
Springfield, VA 22161,

and for the years 1989-1991, from:

Institute of Electrical & Electronics Engineers  
445 Hoes Lane  
Piscataway, NJ 08854.